Role of epigenetics in the pathogenesis of chronic rhinosinusitis with nasal polyps

JONG-YEUP KIM[1,2], DONG-KYU KIM[3], MYEONG SANG YU[4], MIN-JI CHA[1,2], SEONG-LAN YU[5] and JAEKU KANG[5]

[1]Department of Otorhinolaryngology; [2]Myunggok Medical Research Center, College of Medicine, Konyang University, Daejeon 35365; [3]Department of Otorhinolaryngology-Head and Neck Surgery, Chuncheon Sacred Heart Hospital and Institute of New Frontier Research, Hallym University College of Medicine, Chuncheon, Gangwon 24253; [4]Department of Otorhinolaryngology, Konkuk University School of Medicine, Chungju, North Chungcheong 27478; [5]Department of Pharmacology, College of Medicine, Konyang University, Daejeon 35365, Republic of Korea

Received April 26, 2017; Accepted October 26, 2017

DOI: 10.3892/mmr.2017.8001

Abstract. Chronic rhinosinusitis (CRS) is a highly prevalent disease characterized by mucosal inflammation of the nose and paranasal sinuses. CRS can be divided into two main categories, CRS with nasal polyps (NPs; CRSwNP) and CRS without NPs (CRSsNP). Although the pathophysiology of CRS remains unclear, DNA methylation has been implicated in the etiology of CRSwNP. The aim of the present study was to elucidate whether DNA methylation of specific genes is involved in the development of NPs. In total, 18 individuals were included in the present study, and were divided into three groups: CRSwNP (n=7), CRSsNP (n=7) and healthy controls (n=4). NP tissues were obtained from the seven patients with CRSwNP and biopsies of the inferior turbinate mucosa from all three groups were used as controls. Methylated genes detected by methyl-CpG-binding domain sequencing were validated by methylation-specific polymerase chain reaction (PCR), bisulfite sequencing, and reverse transcription-quantitative PCR (RT-qPCR). Methyl-CpG-binding domain sequencing identified 43,674 CpG islands in 518 genes. The promotor regions of 10 and 30 genes were hypermethylated and hypomethylated, respectively, in NP samples compared with controls. The top four genes with altered hypomethylation in NP tissues were, Keratin 19 (*KRT19*), nuclear receptor subfamily 2 group F member 2 (*NR2F2*), A Disintegrin-like And Metallopeptidase (Reprolysin Type) with Thrombospondin type 1 motif 1 (*ADAMTS1*) and zinc finger protein 222 (*ZNF222*). RT-qPCR demonstrated that the expression levels of *KRT19*, *NR2F2* and *ADAMTS1* were significantly increased in NP tissues; however, there was no difference in the levels of *ZNF222* between NP and control tissues. Further studies are required to confirm the relevance of these epigenetic modifications in the mechanisms underlying NP formation.

Correspondence to: Professor Jaeku Kang, Department of Pharmacology, College of Medicine, Konyang University, 158 Gwanjeodong-ro, Seo-gu, Daejeon 35365, Republic of Korea
E-mail: jaeku@konyang.ac.kr

Key words: chronic rhinosinusitis, nasal polyps, chronic rhinosinusitis with nasal polyps, chronic rhinosinusitis without nasal polyps, methylation

Introduction

Chronic rhinosinusitis (CRS), a highly prevalent health condition, is characterized by mucosal inflammation of the nose and paranasal sinuses. CRS is an inflammatory disorder involving the paranasal sinuses and nasal passages which persists for a minimum of 2-3 months, despite attempts at medical management (1-3). Based on the presence and absence of nasal polyps (NPs), CRS is generally divided into two categories, CRS with and CRS without NPs (CRSwNP and CRSsNP, respectively). Although CRSsNP is more prevalent, CRSwNP accounts for approximately 20% of all CRS cases. CRSwNP, which is often accompanied by asthma, fungal rhinosinusitis, and aspirin-exacerbated respiratory disease, is considered more difficult to treat than CRSsNP (4,5). Despite numerous studies, the detailed pathogenic mechanisms underlying NP formation in CRS remain unknown (6).

NPs are a common clinical condition, either in isolation or accompanying CRS. Since 2003, NP formation has been identified as closely related to epigenetic processes. Zheng *et al* (7) identified the top four genes with altered expression in NP samples (*COL18A1*, *EP300*, *GNAS*, and *SMURF1*) from a DNA methylation microarray; these genes were validated as driven by promoter methylation using methylation-specific polymerase chain reaction (PCR). However, unmethylated signals were detected in the promoter regions of *COL18A1*, *EP300*, *GNAS*, and *SMURF1* in all samples. The methylation frequency of *COL18A1* was significantly higher in NPs than in healthy control samples. DNA methylation is a key regulator of gene activity; however, there are many questions regarding this epigenetic mechanism that remain to be answered.

Epigenetics, which generally refers to heritable changes in gene expression and the potential for genetic changes that are not transmitted through alterations in the actual genetic

code (8), has recently been proposed as an explanation for the key gene/environment interactions involved in NP formation (3). The mechanisms of epigenetic regulation underlie many complex diseases and may, therefore, contribute to the development and heritability of paranasal disease (9). North and Ellis (10) recently provided an overview of key studies, indicating an important role for epigenetic modifications in the developmental origins and pathogenesis of atopy and asthma, suggesting the potential for future applications of these research findings to the clinical management of allergy and immunology. Thus, a better understanding of the role of DNA methylation in NP formation is required to inform focused epigenetic studies toward the realization of clinical applications.

As a step toward this goal, the aim of the present study was to identify DNA methylation changes in specific genes potentially important in the pathogenesis of NP. To search for specific genes regulating polyp formation, we performed DNA methylation analysis using a systematic epigenetic regulatory approach. The choice of target genes was based on known epigenetic modulation factors involved in allergies, since changes in the methylation patterns of these is associated with alterations in gene expression, phenotype, and, ultimately, polyp formation. The results of DNA methylation analysis were validated by reverse transcription-quantitative PCR (RT-qPCR), to compare the DNA methylation profiles of genes differentially expressed in patients with CRSwNP and CRSsNP. Our results provide insights into the roles of specific mRNAs as regulators of polyp formation. Moreover, these data could inform the development of therapeutic strategies to modulate the formation of polyps.

Materials and methods

Patients and sample collection. This study was based on data acquired from the Konyang University Hospital (September 2014 to August 2015) through a survey conducted by the Centers for Otorhinolaryngology. The protocol was approved by the Institutional Review Board of Konyang University Hospital (IRB approval no. 2013-01-036), and all individuals provided informed consent prior to inclusion. The diagnosis of CRS was based on the definition of the European Position Paper on Rhinosinusitis and Nasal Polyps 2012 (3). A total of 18 patients were included in the study, divided into three groups: CRSwNP (n=7), CRSsNP (n=7), and healthy controls (n=4). Control tissues were obtained from patients without any sinus disease, with an average age of 47.5 years. Patients with CRSwNP ranged in age from 15 to 66 (average 44.6) years. Seven patients in the CRSwNP group underwent revision sinus surgery. All patients were nonsmokers. Uncinate process (UP) mucosa tissue samples were obtained from control subjects and those with CRSsNP or CRSwNP. NP tissues from patients with CRSwNP were also evaluated. Patients selected for the control group underwent endoscopic transsphenoidal surgery for benign pituitary tumors and did not have symptoms, imaging, or endoscopic findings consistent with CRS.

Exclusion criteria were as follows: i) abnormal atopic status (eosinophil count outside of the normal range and increased immunocap IgE levels); ii) history of smoking; iii) prior treatment with oral or spray steroids for 3 months before surgery; iv) cystic fibrosis, congenital mucociliary problems, systemic vasculitis, gastroesophageal reflux diseases, antrochoanal polyp, and fungal sinusitis. Controls with allergic rhinitis were also excluded. Each tissue sample was divided into two parts, one of which was fixed in 10% formaldehyde and embedded in paraffin for histological analysis, and the other was immediately snap-frozen in liquid nitrogen and stored at -80˚C for future RNA, DNA, and protein extraction. Fresh tissue specimens were quickly cleaned with 0.9% normal saline and sliced into appropriate sections.

HiSeq MBD-seq library preparation. Genomic DNA was extracted from tissue samples using a Maxwell 16 MDx Instrument (Promega Inc., Madison, WI, USA). Each cartridge was placed in a holder with the ridged side of the cartridge facing toward the numbered side of the rack. The plunger was placed in the last well of each cartridge so that the bottom of the plunger reached the bottom of the cartridge. Samples were transferred to the first well, and the cartridge was placed onto the Maxwell 16 platform. The system was run according to the manufacturer protocols and settings for tissue DNA. One microgram of genomic DNA was sheared to 200-400 bp fragments using a Covaris LE220 sonicator (Covaris Inc., Woburn, MA, USA). The resulting fragments were immunoprecipitated using a MethylMiner Methylated DNA Enrichment Kit (Invitrogen), according to the manufacturer's recommended protocol. In brief, methylated DNA was isolated from fragmented whole genomic DNA by binding to the methyl-CpG-binding domain (MBD) of human MBD2 protein, which was coupled to paramagnetic streptavidin beads (Dynabeads M-280) via a biotin linker. Methylated fragments were eluted as a single enriched population using 2 M NaCl elution buffer. Methylated double-stranded DNA was end-repaired (i.e., an 'A' was ligated to the 3' end), and Illumina adapters then ligated to the fragments with a target size of 300-500 bp products. Size-selected products were then PCR-amplified, and validated using an Agilent Bioanalyzer.

Clustering and sequencing. Target gene raw DNA methylation pattern data were extracted as paired files from Illumina software. To further explore molecular variation contributing to the differences between CRSwNP and CRSsNP, we analyzed a flow cell containing millions of unique clusters loaded onto the HiSeq 2000 system for automated cycles of extension and imaging. The Illumina system uses a unique 'bridged' amplification reaction that occurs on the surface of the flow cell. A flow cell containing millions of unique clusters is loaded onto the HiSeq 2000 sequencer for automated cycles of extension and imaging. The Illumina Sequencing-by-Synthesis system utilizes four proprietary nucleotides possessing reversible fluorophore and termination properties. Each sequencing cycle occurs in the presence of all four nucleotides, leading to higher accuracy than methods involving only one nucleotide in the reaction mix at a time. This cycle is repeated, one base at a time, generating a series of images, each representing a single base extension at a specific cluster.

Data processing and methylation profile calling. Paired-end sequencing reads (100 bp) generated by MBD-sequencing were verified for sequence quality using FastQC (version 0.10.0)

and Trimmomatic (version 0.32) was used to remove adapter sequences and bases with quality scores <3 from the reads. In addition, bases that did not meet the criteria, window size ≥4, mean quality score ≥15, were removed using a sliding-window trimming method. Next, reads <36 bp were removed to produce clean data. The cleaned reads were aligned to the human genome (UCSC hg19) using Bowtie (version 1.1.1 parameter set-n 2-m 1-X500) allowing for up to two nucleotide mismatches to the reference genome per seed and returning only uniquely mapped reads. Mapped data (SAM file format) were subjected to sorting and indexing using SAMtools (version 0.1.19). PCR duplicates were removed with Picard Mark Duplicates (version 1.118). Analysis of the MBD data was performed using the MEDIPS package. For each sample, aligned reads were extended in the sequencing direction to 300 nt. The genome-wide sequencing read coverage of extended reads was calculated using a 250 bp window size. The resulting coverage profiles (read count, reads per kilobase of transcript per million mapped reads, root mean square) at each genomic bin were calculated. Each differentially methylated region (DMR) was annotated using the table browser function of the UCSC genome browser. Annotation included gene structures, transcripts, promoter regions (defined as -2 kb upstream of the transcription start site), exons, introns, and CpG islands.

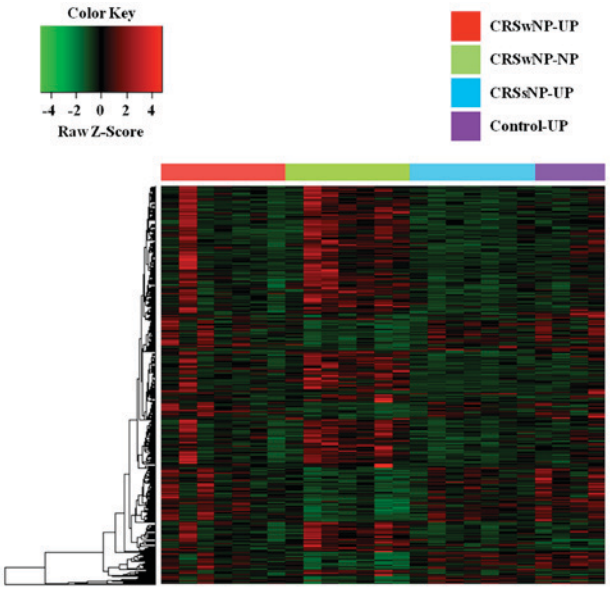

Figure 1. Methyl-CpG-binding domain sequencing of nasal polyp tissue. Data are presented as a heatmap of genes upregulated in CRSwNP-UP, CRSwNP-NP, and CRSsNP-UP tissues vs. Control-UP tissues. CRSwNP, chronic rhinosinusitis with nasal polyps; CRSsNP, chronic rhinosinusitis without nasal polyps; UP, uncinate process mucosa tissue samples; NP, nasal polyps tissue samples.

Identification of DMRs. Read counts at each genomic bin were normalized to the trimmed mean of M-value normalization in the edgeR package. We applied an exact test to assess the significance of methylation differences between comparison groups using edgeR. DMRs were determined by filtering each associated region with a |log2FC|value ≥1 and exact test P<0.05. Hierarchical clustering analysis was also performed using complete linkage and Euclidean distance as a measure of similarity to display the methylation patterns of DMRs that satisfied the significance criteria above for at least one more comparison pair. Gene enrichment and functional annotation analyses were performed using the DAVID tool (http://david.abcc.ncifcrf.gov/home.jsp). All data analysis and visualization of DMRs were conducted using R 3.0.2 (www.r-project.org).

RT-qPCR analysis of mRNAs. Total RNA was isolated from nasal tissues using TRIzol reagent (Ambion) according to the manufacturer's instructions. To estimate mRNA expression levels, cDNAs were synthesized using MMLV reverse transcriptase (Promega). RT-qPCR was performed (in triplicate) using iQTM SYBR Green Supermix and a CFX96 qPCR machine (Bio-Rad, Hercules, CA, USA). The primers used for mRNA detection were as follows: nuclear receptor subfamily 2, group F (*NR2F2*), forward 5'-GCCATAGTCCTGTTCACC TCA-3' and reverse 5'-AATCTCGTCGGCTGGTTGG-3'; *HOXA6*, forward 5'-CGGTTTACCCTTGGATGCA-3' and reverse 5'-GCCCATGGCTCCCATACAC-3'; *ZNF609*, forward 5'-TCCTACCTGCCTTCCAGCTA-3' and reverse 5'-GTGCCT TGTCAGCATCTTCA-3'; *ROBO2*, forward 5'-TGGAGACCT CACAATCACCA-3' and reverse 5'-GGCTGGGCCTTGTAG AATTA-3'; *PDE3A*, forward 5'-GAACAGATGACACTGCTC AAGTT-3' and reverse 5'-GAGCAAGAATTGGTTTGTCCA G-3'; a disintegrin and metalloproteinase with thrombospondin type 1 motif (*ADAMTS1*), forward 5'-TGTGGTGTTTGC GGGGGAAATG-3' and reverse 5'-TCGATGTTGGTGGCT CCAGTT-3'; *KRT19*, forward 5'-CTTCCGAACCAAGTT TGAGAC-3' and reverse 5'-AGCGTACTGATTTCCTCC TC-3'; *ZNF222*, forward 5'-TCAACGAGTCCACACTGG AG-3' and reverse 5'-AGCTCTTCCCGCAGTTATCA-3'; and glyceraldehyde-3-phosphate dehydrogenase (*GAPDH*), forward 5'-ACAGTCAGCCGCATCTTCTT-3' and reverse 5'-ACGACC AAATCCGTTGACTC-3'. The amplification conditions were as follows: a pre-denaturation step at 95˚C for 3 min, followed by 40 cycles of denaturation at 95˚C for 10 sec, annealing at 58˚C for 10 sec, and extension at 72˚C for 10 sec. The $C_{quantification}$ cycle (Cq) comparison method $2^{-\Delta\Delta Cq}$ was used to calculate relative expression levels, with *GAPDH* as the reference gene.

Statistical analysis. Statistical analysis was performed using the MEDIPS (1.16.0) software package. Methylation data analysis and visualization of DMRs was conducted using R 3.0.2 (www.r-project.org). qPCR data are presented as means ± standard deviation. All results were analyzed using Student's t-test. P<0.05 was considered to indicate a statistically significant difference.

Results

Clustering of DNA methylation profiles by Methyl-CpG-binding domain sequencing. DNA methylation profiling, based on unsupervised hierarchical clustering, identified four unique clusters with distinct methylation signatures (Fig. 1). Remarkably, we found that these clusters were correlated with CRS histological subtypes, genetic abnormalities, and clinical outcomes. In our analysis, 10 and 30 genes were significantly hypermethylated and hypomethylated, respectively, in the CRSwNP-NP clusters compared with controls (Table I).

Table I. Genes with altered methylation statuses in nasal polyps.

A, Hyper-methylation

Description	Gene ID	Chromosome	Ensemble accession	Relative levels of methylation			
				Control-UP	CRSsNP-UP	CRSwNP-UP	CRSwNP-NP
Retinitis pigmentosa 1	RP1-202O8.2	1	ENSG00000231868	1.089182[c]	1.440233[c]	0.981016[c]	8.466027
Espin	ESPN	1	ENSG00000187017	0.992249[b]	1.135411[b]	0.907498[b]	6.897929
Microtubule-associated protein 6	MAP6	11	ENSG00000171533	2.217911[a]	2.030746[c]	2.725116[b]	6.570451
MPN domain containing	MPND	19	ENSG00000008382	1.187162[b]	1.589554[b]	2.545118	5.575780
Spindle and kinetochore associated complex subunit 1	SKA1	18	ENSG00000154839	1.851846[a]	1.102924[b]	1.712328[b]	5.197940
STAM binding protein like 1	STAMBPL1	10	ENSG00000138134	1.938985[a]	1.662501[c]	2.256457[b]	5.639432
Rho GTPase activating protein 31	ARHGAP31	3	ENSG00000031081	1.784895[a]	1.671465[c]	2.326500[b]	5.367708
Rho GTPase activating protein 31-antisense RNA 1	ARHGAP31-AS1	3	ENSG00000241155	1.784895[a]	1.671465[c]	2.326500[b]	5.367708
Prostaglandin E receptor 4	PTGER4	5	ENSG00000171522	1.315410[b]	3.022724[b]	3.166246[b]	7.677371
Zinc finger protein 222	ZNF222	19	ENSG00000159885	1.505544[a]	1.383831[a]	1.897399[a]	4.326746

B, Hypo-methylation

Description	Gene ID	Chromosome	Ensemble accession	Relative levels of methylation			
				Control-UP	CRSsNP-UP	CRSwNP-UP	CRSwNP-NP
Pre-mRNA processing factor 31	RP11-120J1.1	9	ENSG00000225472	19.915220[c]	16.500749[c]	15.645956[c]	4.986879
RUN and FYVE domain containing 4	RUFY4	2	ENSG00000188282	16.341624[c]	16.337111[c]	13.857570[c]	5.544202
RUN and FYVE domain containing 5	RUFY5	8	n/a	15.768303[c]	13.305096[c]	11.284723[c]	4.726873
RUN and FYVE domain containing 6	RUFY6	2	n/a	11.826268[c]	9.432234[c]	11.383418[c]	3.242687
RUN and FYVE domain containing 7	RUFY7	8	n/a	13.603286[c]	10.678649[c]	9.672681[c]	4.192238
RUN and FYVE domain containing 8	RUFY8	22	n/a	17.220517[c]	18.166590[c]	16.007680[c]	6.757857
RUN and FYVE domain containing 9	RUFY9	17	n/a	9.348106[c]	11.361693[c]	8.975746[c]	3.930507
RUN and FYVE domain containing 10	RUFY10	8	n/a	10.674316[c]	7.446879[c]	7.634908[c]	2.864527
RUN and FYVE domain containing 11	RUFY11	2	n/a	18.865311[c]	16.251488[c]	13.691127[c]	5.308298
RUN and FYVE domain containing 12	RUFY12	2	n/a	14.840328[c]	11.996467[c]	11.480092[c]	5.715029
RUN and FYVE domain containing 13	RUFY13	11	n/a	14.189715[c]	6.2297629[c]	5.6346066[c]	1.839248
RUN and FYVE domain containing 14	RUFY14	6	n/a	9.701559[c]	7.746522[c]	7.717593[c]	3.025173

Table I. Continued.

B, Hypo-methylation

Description	Gene ID	Chromosome	Ensemble accession	Relative levels of methylation			
				Control-UP	CRSsNP-UP	CRSwNP-UP	CRSwNP-NP
RUN and FYVE domain containing 15	RUFY15	6	n/a	9.701559c	7.746522c	7.717593c	3.025173
RUN and FYVE domain containing 16	RUFY16	10	n/a	8.791565c	7.548554c	6.950384c	2.123994
Doublesex and mab-3 related transcription factor 3	DMRT3	9	ENSG00000064218	8.056680c	6.317158c	6.723381c	2.154214
Nuclear receptor subfamily 2 group E member 1	NR2E1	6	ENSG00000112333	22.525057[c]	16.116569[c]	17.970408[c]	7.319397
Protein tyrosine phosphatase, non-receptor type 3	PTPN3	9	ENSG00000070159	8.833959[c]	6.120884[b]	6.393193[c]	2.302631
Osteopetrosis associated transmembrane protein 1	OSTM1	6	ENSG00000081087	19.509941[c]	14.291747[b]	15.431751[c]	6.735904
Amnion associated transmembrane protein	AMN	14	ENSG00000166126	9.728993[c]	6.652308[b]	8.176856[c]	3.172278
Septin 10	SEPT10	2	ENSG00000186522	18.941045[b]	18.182648[c]	16.404560[b]	8.002855
Zinc finger protein 609	ZNF609	15	ENSG00000180357	9.909624[b]	9.217143[b]	8.947813[b]	4.347291
Family with sequence similarity 196 member A	FAM196A	10	ENSG00000188916	5.235186[a]	5.244315[b]	5.655077[b]	1.967275
Keratin 19	KRT19	17	ENSG00000171345	11.305383[b]	9.410732[b]	4.446763[b]	3.627874
Phosphodiesterase 3A	PDE3A	12	ENSG00000172572	5.004913[b]	3.286156[b]	3.498454[b]	0.721005
Transmembrane protein 132E	TMEM132E	17	ENSG00000181291	3.908044[b]	2.355244[a]	2.723931[b]	0.490595
Ankyrin repeat domain 18A	ANKRD18A	9	ENSG00000180071	3.932660[a]	3.543744[b]	3.043928[a]	1.086252
Nuclear receptor subfamily 2 group F member 2	NR2F2	15	ENSG00000185551	7.370952[a]	5.814443[a]	6.732305[b]	2.443982
Roundabout guidance receptor 2	ROBO2	3	ENSG00000185008	5.092977[a]	4.044153[a]	4.306780[a]	1.735872
ADAM with thrombospondin type 1 motif 1	ADAMTS1	21	ENSG00000154734	3.037976[a]	2.602663[a]	3.056663[b]	0.691831
Solute carrier family 18 member A3	SLC18A3	10	ENSG00000187714	3.300212[a]	2.584836[a]	3.335012[a]	0.991600

[a]P<0.05, [b]P<0.01 and [c]P<0.01 vs. CRSwNP-NP. UP, uncinate process mucosa tissue samples; NP, nasal polyps tissue samples; CRSwNP, chronic rhinosinusitis with NPs; CRSsNP, chronic rhinosinusitis without NPs; n/a, not available.

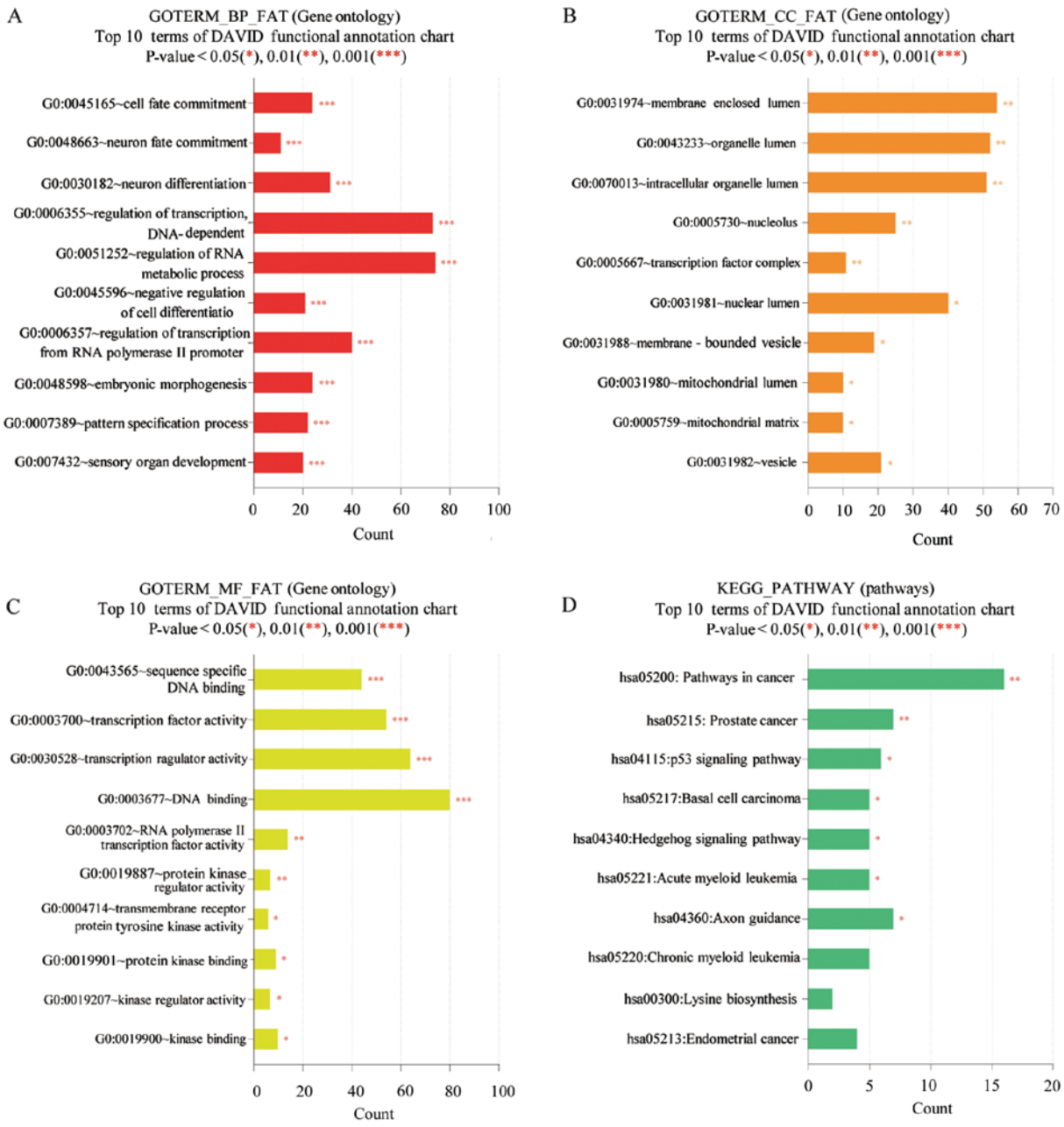

Figure 2. DAVID functional GO analysis of (A) BP, (B) CC, (C) MF and (D) KEGG protein enrichment. *P<0.05, **P<0.01 and ***P<0.001 vs. control. DAVID, Database for Annotation, Visualization and Integrated Discovery; KEGG, Kyoto Encyclopedia of Genes and Genomes; GO, gene ontology; BP, biological processes; CC, cellular components; MF, molecular function.

Functional enrichment analysis. The methylation levels of various genomic features were identified as associated with biological processes occurring at the membrane-enclosed lumen level, particularly in polyp tissue. Gene Ontology analysis indicated that the molecular functions of the majority of the genes identified as differentially methylated were associated with DNA binding and cancer pathways in the Kyoto Encyclopedia of Genes and Genomes pathway database. The results of DAVID analysis are presented in Fig. 2. Functional annotations of proteins encoded by genes in DMRs showing significantly (P<0.05) increased or decreased enrichment compared with controls (Fig. 2) were classified according to their associated biological processes, cellular components, and molecular functions. At the level of biological processes, there were significant differences between proteins encoded by genes in DMRs associated with the cell cycle, cytokinesis, and cell division (Fig. 2A), while analysis of cellular components revealed significant differences between cytoskeletal, vesicular, and synaptic proteins (Fig. 2B). Analysis according to molecular function revealed significant differences between enrichment of encoded proteins associated with translation factor activity, or nucleic acid, spectrin, or enzyme binding (Fig. 2C). At the level of biological processes there were significant differences between enrichment of encoded proteins associated with cell death, intracellular transport, and cellular morphogenesis (Fig. 2D).

Confirmation of gene expression changes by qPCR. For validation of the genetic changes associated with NP formation,

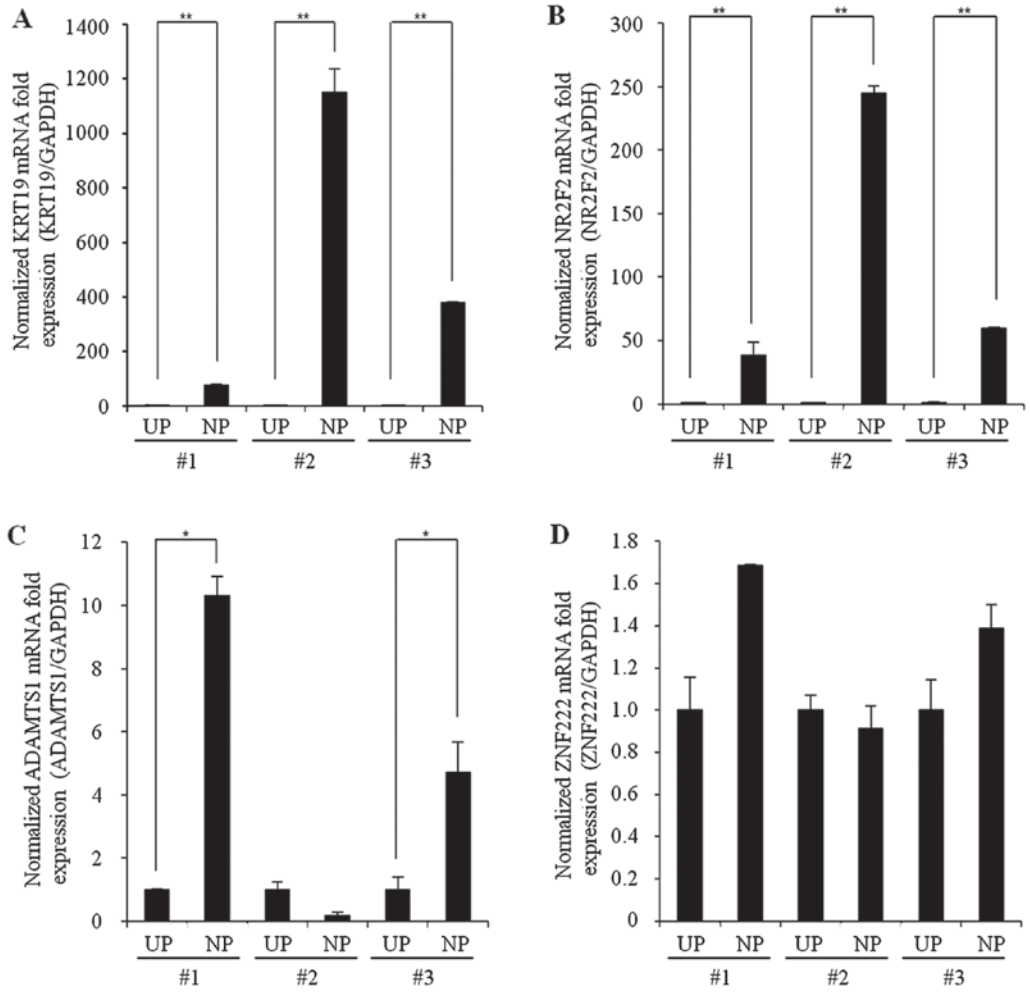

Figure 3. Relative mRNA expression levels of (A) *KRT19*, (B) *NR2F2*, (C) *ADAMTS1* and (D) *ZNF222* in the uncinate process of normal mucosa and nasal polyps determined by reverse transcription-quantitative polymerase chain reaction. Data are presented as the mean ± standard deviation. *P<0.05 and **P<0.01, as indicated. *KRT19*, Keratin 19; *NR2F2*, nuclear receptor subfamily 2 group F member 2; *ADAMTS1*, A Disintegrin-like And Metallopeptidase (Reprolysin Type) with Thrombospondin type 1 motif 1; *ZNF222*, zinc finger protein 222; UP, uncinate process of normal mucosa tissues; NP, nasal polyps tissues.

we evaluated the mRNA expression levels of genes that had previously been reported to be closely related to NP (*KRT19*, *NR2F2*, *ADAMTS1*, and *ZNF222*) in samples from three patients with CRSwNP using qPCR. The mRNA expression levels of *KRT19* and *NR2F2* were significantly increased in samples from all three patients with CRSwNP (CRSwNP-NP) compared with UP control samples (Control, CRSsNP-UP, and CRSwNP-UP) (Fig. 3A and B); however, although the mRNA expression level of *ADAMTS1* was significantly increased in two of the patients, the other patient showed no significant difference in expression from controls. *ZNF222* mRNA levels did not differ significantly between the NP and UP tissues from any patients.

Discussion

Recent studies have identified genes of unknown function that are associated with disease as also related to NP growth. Fritz *et al* (11) examined 12,000 human genes transcribed in the nasal mucosa of patients with allergic rhinitis with and without NP, and identified 34 differentially expressed genes, including those encoding inflammatory molecules and putative growth factors. Specifically, the expression levels of 16 genes were increased, and those of 18 genes were decreased in the polyp group. Although genetic studies based on comparisons with a control group to evaluate epigenetic changes, gene rearrangement, and changes in chromatin structure. have been performed for patients with NPs, the results have been inconsistent. This may be due to heterogeneity among experimental groups or genetic differences among the ethnic groups included in the studies; however, the major cause of such variation is expected to be environmental influences on the regulation of polyp-related genes (7). Indeed, there is a growing body of literature suggesting a role for epigenetic factors in the complex interplay between genes and the environment (12,13). DNA methylation is a key to regulation of the genes responsible for polyps; however, the details of the mechanisms involved remain poorly understood.

To investigate genes differentially transcribed in the nasal mucosa of patients with allergic rhinitis with and without nasal polyps, we conducted systematic gene expression profiling experiments using clinical samples to identify genes involved in polyp formation. Genomic methylation and expression analysis of target genes were performed on tissues from patients with CRSsNP and CRSwNP. To the best of our knowledge, this is the first study to use epigenetic technology

to quantitatively and simultaneously monitor the expression and DNA methylation status of genes involved in allergic rhinitis with and without NP.

In this study, the methylation levels of 19,256 genes were analyzed in CRSwNP-UP, CRSsNP-UP, and control-UP samples compared with those in CRSwNP-NP samples. Among these genes, 518 exhibited differential methylation, primarily those functionally characterized as related to inflammation. Several DNA methylation patterns were similarly regulated in the CRSwNP-UP, CRSsNP-UP, and control-UP samples compared with the CRSwNP-NP samples. These results confirm that the UP mucosa can be a suitable control tissue for epigenetic studies. Indeed, the UP mucosa is one of the common sites of NP development. Moreover, our results support the findings of previous studies of differences in innate immune cells during disease progression in non-asthmatic CRS patients by comparison of the UP mucosa and NPs (14,15).

Patients without any nasal or sinus disease were recruited as a control group to detect differences between NP tissue and healthy nasal mucosa. Validation of the expression levels of genes exhibiting differences in methylation patterns between the groups revealed that the expression levels of *KRT19*, *NR2F2*, and *ADAMTS1* were significantly different between the CRSwNP-NP and UP mucosa (Control-UP, CRSwNP-UP, and CRSsNP-UP) tissues. This represents the first demonstration of the direct involvement of a translational regulation mechanism in polyp formation. The detected P-value could be used for quality control of the data. In this study, 10 and 30 genes were found to be hypermethylated and hypomethylated, respectively, in CRSwNP-NP compared with UP mucosa tissue samples.

Previous studies have also indicated that the genetics of NP formation may be affected by environmental factors (7). Treatment with local glucocorticoids is generally prescribed to alleviate the symptoms of NPs. Benson *et al* (16) identified altered expression of 203 genes between patients treated with glucocorticoids compared with those who did not receive glucocorticoid treatment; 54 genes were downregulated, and 85 upregulated in the glucocorticoid-treated group. Of the 139 genes with known functions, 22 pro-inflammatory genes were downregulated, and a number of anti-inflammatory genes were found to be upregulated in the glucocorticoid-treated group. In addition, hypomethylation of the phosphodiesterase (*PDE*) gene was detected in the polyp group in this study. Similar to the present study, the expression levels of *NR2F2* and *ADAM28* were among those that increased after glucocorticoid treatment, and these were also identified as hypomethylated using methyl-CpG-binding domain sequencing.

Esselens *et al* (17) studied the potential of *Staphylococcus aureus* enterotoxin B to induce changes in the gene DNA methylation pattern in inflamed nasal tissue. They generated a list of 43 genes exhibiting altered methylation states after 24 h of culture with *S. aureus* enterotoxin B; 33 genes were hypermethylated (including *ROBO1*, *FAM59A*, *SLC25A24*, *TMEM138*, *ADAMTS16*, and *ZNF541*) and 10 were hypomethylated (including *ANKRD18A*, *ROBO2*, *FAM196A*, *SLC18A3*, *TMEM132E*, *ADAMTS1*, and *ZNF609*). *ADAMTS1*, encoding a matrix metalloprotease, was also found to be differentially methylated in the present study. The ADAMTS1 protein is involved in modification of the extracellular matrix, and also acts as an inhibitory protein present in neural scars that cleaves extracellular matrix proteins.

Moreover, differential methylation patterns were detected in a genome-wide analysis of polyp tissue from patients with aspirin-intolerant asthma compared with aspirin-tolerant asthma; hypermethylation was detected at 332 loci in 296 genes, while hypomethylation was detected at 158 loci in 141 genes (18). Gene ontology analysis revealed that the hypomethylated genes were involved in cell communication, proliferation, cytokine biosynthesis, cytokine secretion, immune responses, inflammation, and immunoglobulin binding, whereas the hypermethylated genes were involved in ectoderm development, hemostasis, wound healing, calcium ion binding, and oxidoreductase activity. The genes *KRT4*, *KRT5*, *KRT8*, *KRT15*, *KRT19*, and *KRT24* were hypomethylated and enriched in biological pathways (19). Our results confirmed that *KRT19* was hypomethylated in polyp tissue.

In the present study, the zinc-finger protein genes *ZNF609* and *ZNF22* were identified as hypomethylated and hypermethylated in NP tissue, respectively. Similarly, patients with allergic fungal sinusitis exhibited expression differences in 10 genes, including *ZNF146* (20). Among the other genes identified as hypomethylated in polyps, those of the *RUFY* gene family were particularly highly expressed. *RUFY4* is involved in metal ion and protein binding. This is the first report of an association of a member of the *RUFY* gene family with NPs; further studies are required to confirm whether other members of this family have roles in polyp formation.

The aim of this study was to detect differences in DNA methylation patterns between patients with CRS with and without NPs. Although we detected clear differences, they were subtle, and involved only a few characters. In addition, only a few differences in gene expression were identified between the groups, and we were unable to distinguish between NP subtypes, such as eosinophilic and neutrophilic. Nevertheless, this study confirmed that epigenetic variation has a major role in the formation of polyps. While our study provides baseline reference data indicating a role for methylation in polyp formation and the candidate genes involved, more studies with larger sample sizes are clearly needed to better elucidate the mechanisms of formation and epigenetics of polyps. In particular, further studies should focus on the specific roles of the *KRT19*, *NR2F2*, and *ADAMTS1* genes on NP development, and on other genes identified as demonstrating differential methylation patterns in this study.

Acknowledgements

The present study was supported by the Basic Science Research Program through the National Research Foundation of Korea (NRF), funded by the Ministry of Education, Science and Technology (grant nos. 2016R1C1B2012384 and 2015R1D1A3A01019948).

References

1. Casale M, Pappacena M, Potena M, Vesperini E, Ciglia G, Mladina R, Dianzani C, Degener AM and Salvinelli F: Nasal polypsosis: From pathogenesis to treatment, an update. Inflamm Allergy Drug Targets 10: 158-163, 2011.

2. Hamilos DL: Chronic rhinosinusitis: Epidemiology and medical management. J Allergy Clin Immunol 128: 693-709, 2011.
3. Fokkens WJ, Lund VJ, Mullol J, Bachert C, Alobid I, Baroody F, Cohen N, Cervin A, Douglas R, Gevaert P, *et al*: European position paper on rhinosinusitis and nasal polyps 2012. Rhinol Suppl 3: 1-298, 2012.
4. Dykewicz MS and Hamilos DL: Rhinitis and sinusitis. J Allergy Clin Immunol 125: S103-S115, 2010.
5. Chaaban MR, Walsh EM and Woodworth BA: Epidemiology and differential diagnosis of nasal polyps. Am J Rhinol Allergy 27: 473-478, 2013.
6. Alexiou A, Sourtzi P, Dimakopoulou K, Manolis E and Velonakis E: Nasal polyps: Heredity, allergies, and environmental and occupational exposure. J Otolaryngol Head Neck Surg 40: 58-63, 2011.
7. Zheng YB, Zhao Y, Yue LY, Lin P, Liu YF, Xian JM, Zhou GY and Wang DY: Pilot study of DNA methylation in the pathogenesis of chronic rhinosinusitis with nasal polyps. Rhinology 53: 345-352, 2015.
8. Hamilos DL: Chronic rhinosinusitis patterns of illness. Clin Allergy Immunol 20: 1-13, 2007.
9. Slavin RG, Spector SL, Bernstein IL, Kaliner MA, Kennedy DW, Virant FS, Wald ER, Khan DA, Blessing-Moore J, Lang DM, *et al*: The diagnosis and management of sinusitis: A practice parameter update. J Allergy Clin Immunol 116 (6 Suppl): S13-S47, 2005.
10. North ML and Ellis AK: The role of epigenetics in the developmental origins of allergic disease. Ann Allergy Asthma Immunol 106: 355-362, 2011.
11. Fritz SB, Terrell JE, Conner ER, Kukowska-Latallo JF and Baker JR: Nasal mucosal gene expression in patients with allergic rhinitis with and without nasal polyps. J Allergy Clin Immunol 112: 1057-1063, 2003.
12. White GP, Hollams EM, Yerkovich ST, Bosco A, Holt BJ, Bassami MR, Kusel M, Sly PD and Holt PG: CpG methylation patterns in the IFNgamma promoter in naive T cells: Variations during Th1 and Th2 differentiation and between atopics and non-atopics. Pediatr Allergy Immunol 17: 557-564, 2006.
13. Baron U, Floess S, Wieczorek G, Baumann K, Grützkau A, Dong J, Thiel A, Boeld TJ, Hoffmann P, Edinger M, *et al*: DNA methylation in the human FOXP3 locus discriminates regulatory T cells from activated FOXP3(+) conventional T cells. Eur J Immunol 37: 2378-2389, 2007.
14. Fokkens W, Lund V, Bachert C, Clement P, Helllings P, Holmstrom M, Jones N, Kalogjera L, Kennedy D, Kowalski M, *et al*: EAACI position paper on rhinosinusitis and nasal polyps executive summary. Allergy 60: 583-601, 2005.
15. Meltzer EO, Hamilos DL, Hadley JA, Lanza DC, Marple BF, Nicklas RA, Bachert C, Baraniuk J, Baroody FM, Benninger MS, *et al*: Rhinosinusitis: Establishing definitions for clinical research and patient care. J Allergy Clin Immunol 114 (6 Suppl): S155-S212, 2004.
16. Benson M, Carlsson L, Adner M, Jernås M, Rudemo M, Sjögren A, Svensson PA, Uddman R and Cardell LO: Gene profiling reveals increased expression of uteroglobin and other anti-inflammatory genes in glucocorticoid-treated nasal polyps. J Allergy Clin Immunol 113: 1137-1143, 2004.
17. Esselens C, Malapeira J, Colomé N, Casal C, Rodríguez-Manzaneque JC, Canals F and Arribas J: The cleavage of semaphorin 3C induced by ADAMTS1 promotes cell migration. J Biol Chem 285: 2463-2473, 2010.
18. Cheong HS, Park SM, Kim MO, Park JS, Lee JY, Byun JY, Park BL, Shin HD and Park CS: Genome-wide methylation profile of nasal polyps: Relation to aspirin hypersensitive in asthmatics. Allergy 66: 637-644, 2011.
19. Sridhar S, Schembri F, Zeskind J, Shah V, Gustafson AM, Steiling K, Liu G, Dumas YM, Zhang X, Brody JS, *et al*: Smoking-induced gene expression changes in the bronchial airway are reflected in nasal and buccal epithelium. BMC Genomics 9: 259, 2008.
20. Orlandi RR, Thibeault SL and Ferguson BJ: Microarray analysis of allergic fungal sinusitis and eosinophilic mucin rhinosinusitis. Otolaryngol Head Neck Surg 136: 707-713, 2007.